Open-ocean carbon monoxide photoproduction

Aron Stubbins[a,*,1], Günther Uher[a], Cliff S. Law[b,2], Kenneth Mopper[c],
Carol Robinson[b], Robert C. Upstill-Goddard[a]

[a]*School of Marine Science and Technology, University of Newcastle-upon-Tyne, Newcastle NE1 7RU, UK*
[b]*Plymouth Marine Laboratory, West Hoe, Plymouth PL1 3DH, UK*
[c]*Department of Chemistry and Biochemistry, Old Dominion University, Norfolk, VA 23529, USA*

Abstract

Sunlight-initiated photolysis of chromophoric dissolved organic matter (CDOM) is the dominant source of carbon monoxide (CO) in the open-ocean. A modelling study was conducted to constrain this source. Spectral solar irradiance was obtained from two models (GCSOLAR and SMARTS2). Water-column CDOM and total light absorption were modelled using spectra collected along a Meridional transect of the Atlantic ocean using a 200-cm pathlength liquid waveguide UV-visible spectrophotometer. Apparent quantum yields for the production of CO (AQY_{CO}) from CDOM were obtained from a parameterisation describing the relationship between CDOM light absorption coefficient and AQY_{CO} and the CDOM spectra collected. The sensitivity of predicted rates to variations in model parameters (solar irradiance, cloud cover, surface-water reflectance, CDOM and whole water light absorbance, and AQY_{CO}) was assessed. The model's best estimate of open-ocean CO photoproduction was 47 ± 7 Tg CO-C yr^{-1}, with lower and upper limits of 38 and 84 Tg CO-C yr^{-1}, as indicated by sensitivity analysis considering variations in AQYs, CDOM absorbance, and spectral irradiance. These results represent significant constraint of open-ocean CO photoproduction at the lower limit of previous estimates. Based on these results, and their extrapolation to total photochemical organic carbon mineralisation, we recommend a downsizing of the role of photochemistry in the open-ocean carbon cycle.
© 2006 Elsevier Ltd. All rights reserved.

Keywords: Carbon monoxide; Dissolved organic matter; Photochemistry; Open-ocean; Carbon cycling; Atlantic Meridional Transect

1. Introduction

Carbon monoxide (CO) is the second largest identified product of marine dissolved organic matter (DOM) photolysis (Miller and Zepp, 1995; Mopper and Kieber, 2000). First evidence for a predomi-nantly photochemical CO source in seawater came from observations of a pronounced diurnal cycle in sea-surface CO concentrations. These observations were later explained by the interplay between a strong photoproduction term (Wilson et al., 1970; Conrad et al., 1982; Redden, 1982; Bullister et al., 1982; Gammon and Kelly, 1990; Zuo and Jones, 1995; Zafiriou et al., 2003) and fast removal by microbial oxidation (Conrad and Seiler, 1980, 1982; Zafiriou et al., 2003), although air–sea gas exchange (Conrad et al., 1982; Conrad and Seiler, 1982; Erickson, 1989; Bates et al., 1995; Zuo and Jones,

*Corresponding author. Tel.: +1 757 515 8778.

E-mail addresses: aron.stubbins@gmail.com, ron.stubbins@gmail.com (A. Stubbins).

[1]Now at Department of Chemistry and Biochemistry, Old Dominion University, Norfolk, VA 23529, USA.

[2]Now at NIWA, PO Box 14 901, Wellington, New Zealand.

1995; Stubbins et al., 2006) and downward mixing (Kettle, 1994, 2005; Doney et al., 1995; Najjar et al., 1995; Gnanadesikan, 1996; Johnson and Bates, 1996) also may be important. These interactions between biogeochemical and physical processes lead to complex spatial and temporal patterns in CO cycling that still pose a challenge today. After four decades of research into CO photoproduction, the photochemical source term still remains poorly constrained (for recent review see, Zafiriou et al., 2003) with estimates covering more than two orders of magnitude, ranging from 30 to 820 Tg CO-C yr^{-1} (Valentine and Zepp, 1993; Zuo and Jones, 1995; Moran and Zepp, 1997; Siegel, 2001; Zafiriou et al., 2003). The significance of photochemical CO production and the uncertainty in recent estimates is best illustrated by comparison with other carbon cycle terms. For example, estimates of the photochemical CO source are equivalent to 8–200% of global riverine DOM inputs (Prather et al., 2001) and 16–350% of carbon burial in marine sediments (Hedges et al., 1997). These comparisons clearly illustrate the importance of CO photoproduction and the requirement to constrain further its potential contribution to carbon cycling.

Precise and accurate quantification of CO photo-production rates is facilitated by the availability of sensitive analytical techniques and low CO back-ground levels, making CO photoproduction one of the most thoroughly studied environmental photo-reactions. For this reason CO has been suggested as a proxy for the production of both dissolved inorganic carbon (Miller and Zepp, 1995; Gao and Zepp, 1998; Johannessen et al., 2000; Mopper and Kieber, 2000) and biolabile organic carbon (Kieber et al., 1989; Miller and Moran, 1997; Moran and Zepp, 1997; Miller et al., 2002b), which together account for the majority of DOM photodegradation products. Current best estimates of the combined strength of the dissolved organic carbon sink associated with DOM photodegradation are in the order of 10–30% of global oceanic primary production (Miller and Moran, 1997; Mopper and Kieber, 2000), clearly relevant on Global scales. Further-more, CO has also emerged as a key tracer for use in testing and tuning models of other mixed-layer processes, including photochemistry, ocean optics, radiative flux, mixing and air–sea gas exchange (Kettle, 1994, 2005; Doney et al., 1995; Najjar et al., 1995; Gnanadesikan, 1996; Johnson and Bates, 1996). Hence, improved modelling and quantifica-

tion of marine CO photoproduction will contribute to our understanding of a variety of interconnected marine biogeochemical processes.

In this paper, we present a model of CO photoproduction using spectral data for solar irradiance, coloured DOM (CDOM), and whole water absorbance, and apparent quantum yields of CO formation. The study utilises the SMARTS2 model to calculate surface irradiance, providing increased accuracy and precision, and greater spectral coverage (280–800 nm) and resolution (1 nm), compared to the GCSOLAR model. Open-ocean CDOM spectra were collected using a 200-cm pathlength spectrophotometer, providing increased sensitivity and precision compared to traditional 10-cm pathlength spectrophotometers, particularly at wavelengths >360 nm. These two refinements en-abled us to model more accurately the initiation process in the photoproduction of CO, namely the absorbance of sunlight by CDOM in the water column. Thorough sensitivity analyses were con-ducted to determine the impact of any potential errors in the model's input data and underlying assumptions. We discuss our results in the context of present knowledge of the biogeochemical cycling of open-ocean CO and briefly comment upon implications for the marine dissolved organic carbon cycle.

2. Methods

2.1. Study area

Open-ocean CDOM light absorption spectra (Section 2.2.2) were collected during the open-ocean section of the 15th cruise of the Atlantic Meridional Transect programme (AMT-15) aboard R.R.S. *Discovery* (Fig. 1). The cruise departed South-ampton, UK (51°N, 1°W), on 17/09/2004 and arrived in Cape Town, South Africa (34°S, 18°E), on 31/10/2004, and its open-ocean section extended from 22°N, 18°W to 39°S, 02°W, transecting the intertropical convergence zone (ITCZ), equator (25°W) and the southern gyre. Other data used in this study were obtained from parameterisations and modelling approaches as described in detail below.

2.2. Model rationale

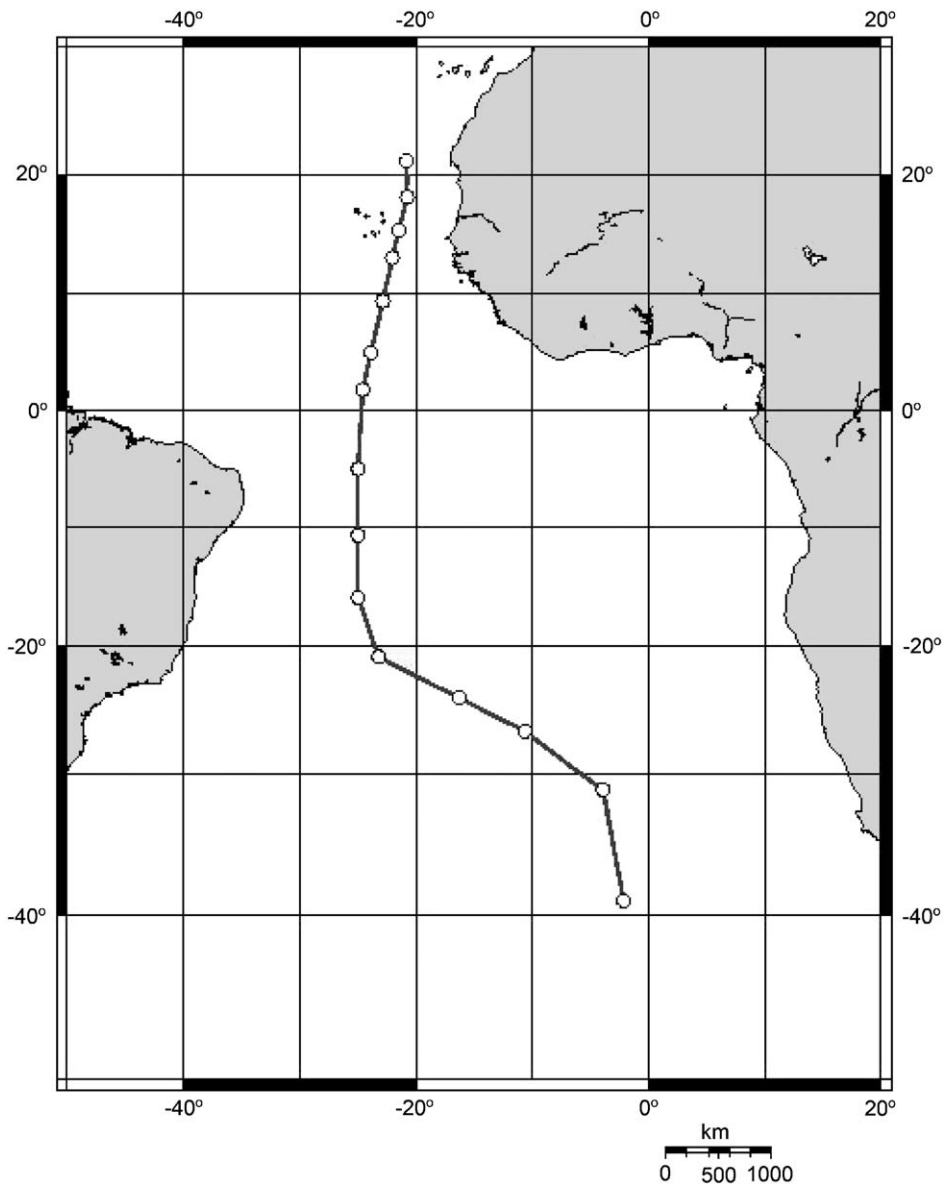CO photoproduction rates were calculated as the quanta of photons absorbed by CDOM multiplied

Fig. 1. Open-ocean portion of AMT-15 cruise track during which 199 total water and coloured dissolved organic matter spectra were collected.

by the apparent quantum yield of CO, AQY_{CO}, over the relevant wavelength (λ) range (280–800 nm, adapted from Zafiriou et al., 2003):

$$\sum_{\text{Ocean area}} \int_{280}^{800} (\text{irradiance} \times \text{attention}_{1+2}$$
$$\times A_{\text{CDOM}}/A_{\text{Total}}[1 - 10^{-A_{\text{CDOM}}}]AQY_{CO})_{\lambda}, \qquad (1)$$

where irradiance is global spectral solar irradiance (Section 2.2.1), attenuation factors 1 and 2 are corrections for the reflection of light by cloud (0.8; Nelson et al., 1998; Zafiriou et al., 2003) and water surface albedo (non-spectral, 0.93; Zepp and Cline, 1977), and A_{CDOM} and A_{Total} are the CDOM and total light absorption (optical density) in the water column (Section 2.2.2).

2.2.1. Solar irradiance within surface waters

Two sets of spectral solar irradiance data were used for comparison. The first data set (Leifer, 1988) covers wavelengths from 297.5 to 800 nm and was derived from the GCSOLAR model (Zepp and Cline, 1977). However, these data are surface

irradiance multiplied by ln(10), a correction made for their intended use in modelling photoreactions in very weakly absorbing systems (i.e. systems where only a small fraction of light is absorbed ($A < 0.02$) due to very low levels of chromophores combined with shallow depths). As the current application does not meet these criteria, due to greater than intended depths, these data were converted back to irradiance at the water's surface ($\div 2303$; for full discussion see Leifer, 1988). Whilst this data set is readily available in a convenient form, it does not cover the full range of solar irradiance involved in photoreactions, and is limited in terms of spectral, temporal and geographic resolution. A more recent model, SMARTS2 (Gueymard, 1995), covering the full range of photochemically active radiation (280–800 nm) and with a spectral resolution of 1 nm, was considered to better estimate solar irradiance. SMARTS2 is available as an Excel interface (http://rredc.nrel.gov/solar/models/SMARTS/) with 30 user-defined parameters, and provides accuracy and precision comparable to more complex, computer intensive simulations such as MODTRAN4 (Myers et al., 2002). SMARTS2 output data are available in the form of direct, diffuse and global solar irradiance at the Earth's surface (global in this case refers to irradiance integrated over the entire hemisphere of the sky and over the whole solar spectrum, not to "whole Earth") in photons $cm^{-1} s^{-1} nm^{-1}$. Fig. 2 compares the SMARTS2 output to direct spectral irradiance at noon on a cloudless day over the North Atlantic Ocean (1 July 2002; Latitude 39°N, Longitude 75°S) as measured using an Optronics Spectroradiometer on board R.V.S. *Endeavor*. SMARTS2 can be seen to predict accurately and precisely variations in direct solar irradiance at wavelengths < 450 nm. Above 450 nm the model over estimates irradiance by ~10%. Open-ocean atmosphere parameters were used to estimate irradiance; therefore the proximity to land and commercial aircraft flight paths (USA, eastern seaboard) of the direct measurement is the likely cause for the models overestimation. In any case such an overestimate at wavelengths > 450 nm will be of limited significance, as photoreactions involving CDOM are predominantly driven by shorter wavelengths. Global irradiance was also slightly higher than direct irradiance as it also includes the diffuse component (Fig. 2). The detail in the inset in Fig. 2 shows that the modelled data are more realistic than the measured data in the UV-B between 290 and 295 nm, where commercial spectroradiometers have a tendency to overestimate light levels (Gueymard, 1995). Average daily spectral global irradiance was generated at 0°, 10°, 20°, 30°, 40°, 50°, 60°, 70° and 80° latitude, North and South, for the winter and summer solstices, spring and winter equinoxes, and mid-points between each,
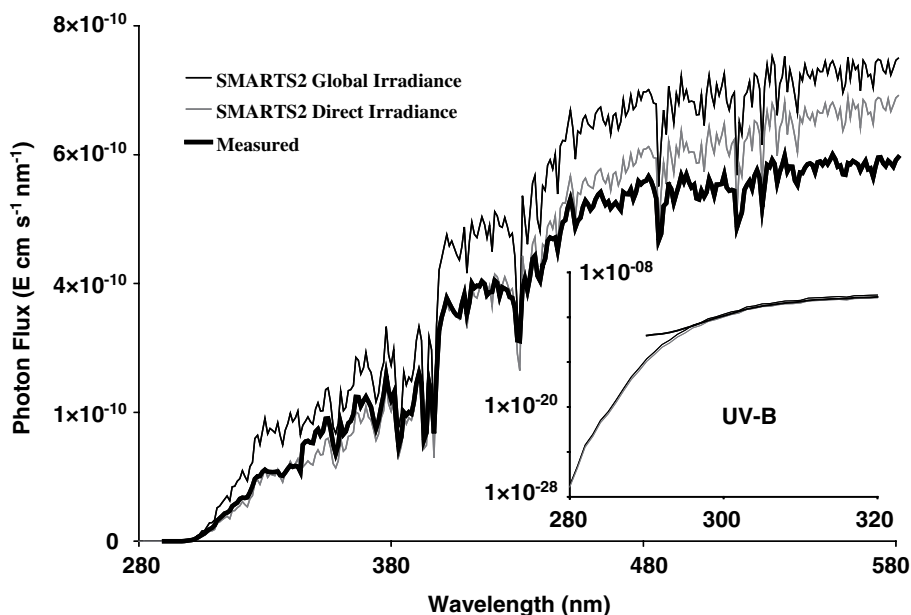

Fig. 2. Modelled (SMARTS2) direct and global solar irradiance and measured direct solar irradiance (Optronics Spectroradiometer; Andrew Davis and Emily White, personal communication). UV-B inset is the same data on a logarithmic scale.
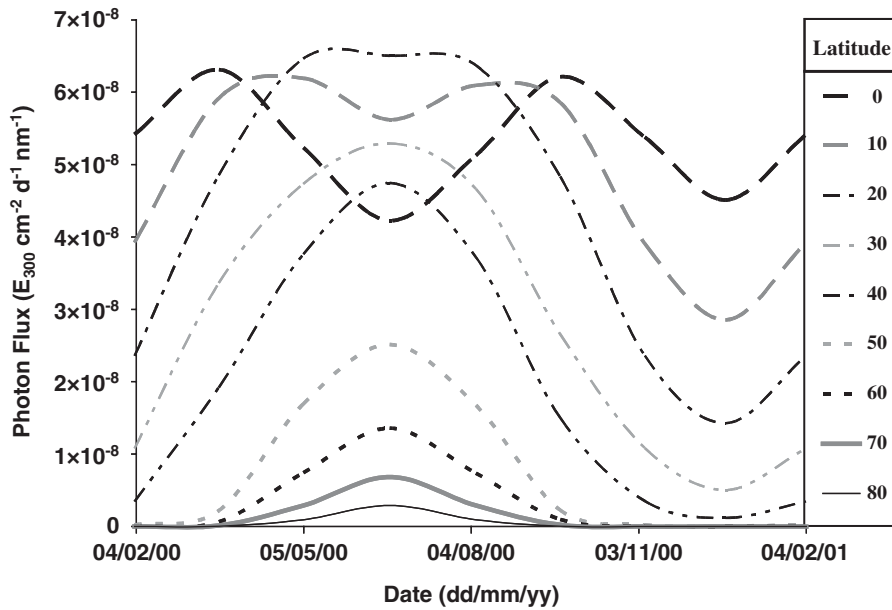
Fig. 3. Seasonal variation in modelled (SMARTS2) daily solar irradiance (300 nm) with latitude.

giving a total of eight equidistant dates. Fig. 3 shows the calculated seasonal variations in irradiance at 300 nm with latitude. Similar graphs were constructed at a wavelength resolution of 1 nm over the spectral range 280–800 nm and the areas under the curves calculated by integration (SPSS Sigmaplot) to determine annual irradiance at each wavelength at each 10° latitudinal band. (Data available through the British Oceanographic Data Centre (BODC); http://www.bodc.ac.uk/projects/uk/amt/data_inventories/, AMT-15, Aron Stubbins, file name "SMARTS2 Irradiance 10-deg Latitudinal Bands.xls".) Both sets of spectral irradiance data were extrapolated to the Global ocean area using 10° latitudinal band surface areas obtained from Caires and Sterl (2005).

2.2.2. Light absorption in the water column

The level of light absorption was calculated for the entire photic zone (no specific depth implied) assuming that all light is absorbed by CDOM, particulates and water. A_{CDOM} was calculated using the mean spectral absorption coefficient, a (m^{-1}) spectrum of 199 open-ocean surface-water CDOM spectra collected during AMT-15 (Fig. 4 and Table 1) using a 200-cm pathlength waveguide spectrophotometer (WPI Inc., model UltraPath-UV). Samples were filtered using 0.1-μm filter cartridges (Whatman, Polycap 75 TF), which were soaked
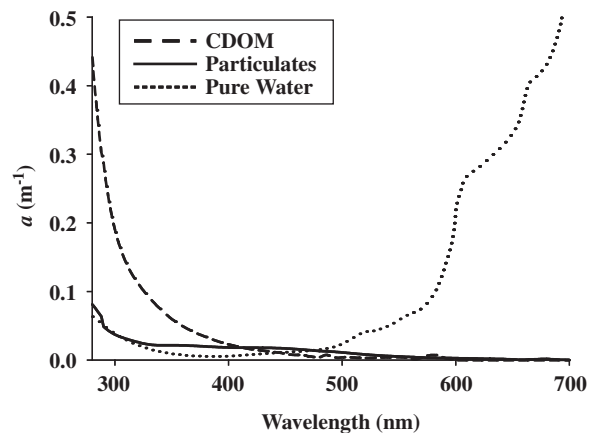

Fig. 4. Light absorption spectra for major chromophoric constituents of seawater. Coloured dissolved organic matter (CDOM) is the Atlantic Ocean mean from AMT-15 (199 samples, measured using a 200 cm pathlength waveguide spectrophotometer (WPI UV-UltraPath), Autumn 2004). Particulate absorption is the Atlantic Ocean mean AMT-15 (difference between filtered and unfiltered samples 199, measured using a 200 cm pathlength waveguide spectrophotometer). Pure water spectra from Buiteveld et al. (1994).

(1–2 days) in acetonitrile, back-flushed and then rinsed with copious volumes of pure laboratory water (Millipore, Milli-Q 185 plus, hereafter referred to as Milli-Q) until the difference in a of filtered and unfiltered Milli-Q was $<0.001\,\mathrm{m}^{-1}$ at 300 nm. Filters were used for 1 day before

Table 1
Mean light open-ocean coloured dissolved organic matter (CDOM) and particulate absorption coefficients (a)

Wavelength (nm)	CDOM a (m^{-1}) $\pm$ standard deviation	Particulate a (m^{-1}) $\pm$ standard deviation
260	0.856 + 0.0763	0.154 + 0.0659
280	0.444 + 0.0547	0.101 + 0.0585
300	0.190 + 0.0297	0.0567 + 0.0408
320	0.113 + 0.0231	0.0457 + 0.0380
340	0.0743 + 0.0171	0.0411 + 0.0356
360	0.0489 + 0.0091	0.0409 + 0.0323
380	0.0336 + 0.0059	0.0393 + 0.0311
400	0.0228 + 0.0045	0.0379 + 0.0305
420	0.0157 + 0.0035	0.0376 + 0.0302
440	0.0113 + 0.0026	0.0371 + 0.0299
460	0.0075 + 0.0020	0.0354 + 0.0294
510	0.0036 + 0.0012	0.0291 + 0.0279
560	0.0021 + 0.0011	0.0240 + 0.0269
610	0.0006 + 0.0001	0.0220 + 0.0262

Data represent the mean of 199 open-ocean surface-water samples collected during AMT-15 (2004).

re-cleaning; four such filters were used during the cruise to allow for this cycle of use and cleansing, and to provide backup in case of filter blockage or failure. Due to strong refractive index effects, it was not possible to use Milli-Q water as a blank (Miller et al., 2002a). Instead sodium chloride solutions were used as blanks. These were prepared from reagent grade NaCl, baked at $400\,^{\circ}C$ to remove organics and dissolved in Milli-Q water to provide solutions close to sample salinity ($\pm 1\,g\,L^{-1}$). All other sample handling and methodology were adapted from Miller et al. (2002a). This CDOM spectrum was chosen due to our confidence in filtration blanks and the high sensitivity of this long pathlength instrument, particularly important above 350 nm where CDOM a in the open-ocean ($<0.05\,m^{-1}$, AMT-15 cruise average) begins to reach the detection limit of conventional 10-cm cuvette spectrophotometers ($0.046\,m^{-1}$, Kitidis et al., 2006). A_{Total} was the total light absorption in the water column, calculated as the sum of CDOM (Fig. 4, AMT-15 mean CDOM), pure water (Fig. 4, Buiteveld et al., 1994) and particulate absorbance spectra (Fig. 4 and Table 1). The particulate absorbance spectra adopted for this work was determined from the difference of unfiltered, whole water absorbance minus filtered-water absorbance averaged over 199 samples collected during AMT-15 using the UltraPath-UV. Except for filtration,

whole water absorbance measurements followed the same procedures. The 199 CDOM and whole water absorbance spectra collected during AMT-15 are available through the BODC website (http://www.bodc.ac.uk/projects/uk/amt/data_inventories/, AMT-15, Aron Stubbins, file name "AMT15 Surface CDOM for BODC.xls").

2.2.3. CO apparent quantum yields

The efficiency of an environmental photoreaction involving CDOM is usually described by its apparent quantum yield, i.e. the ratio of moles of photoproduct formed (in this case CO) to moles of photons (Einstein's, E) absorbed by the chromophore, CDOM (Leifer, 1988). The term apparent is used in reference to the unknown nature and concentration of the specific chromophores involved. AQY_{CO} spectra were constructed using parameterisations describing the AQY_{CO} in terrestrial, estuarine and marine waters as a function of wavelength and CDOM absorption coefficient (Stubbins, 2001). Therefore, the successful use of these parameterisations relies on the availability of accurate CDOM spectra for specific geographical regions. Here, we used the mean Atlantic Ocean CDOM spectrum calculated from 199 surface CDOM spectra collected during AMT-15 using the 200 cm UV-UltraPath spectrophotometer (Fig. 4 and Table 1). The rationale (greater sensitivity and confidence in filtered samples) for the use of this spectrum were discussed above. The resultant AQY_{CO} spectrum (Fig. 5) was both quantitatively and spectrally similar to previous AQY_{CO} determinations for oceanic waters (Fig. 5). However, above 360 nm our calculated apparent quantum yields were slightly higher than those reported by Zafiriou et al. (2003) and Ziolkowski (2000) (Fig. 5). This was attributed to two factors. Firstly, determining CDOM absorbance in oceanic waters using traditional 10-cm quartz cuvettes (as used in Ziolkowski, 2000 and Zafiriou et al., 2003) leads to significant errors when determining light absorption at wavelengths >360 nm. Kitidis et al. (2006) quote instrument precision and detection limits for their double beam spectrophotometers with 10-cm cuvettes as 0.023 and $0.046\,m^{-1}$, respectively. Assuming these values are representative of other conventional spectrophotometers using 10-cm cuvettes, the AMT-15 CDOM spectra (Fig. 4 and Table 1) measured using the UV-UltraPath (200 cm) show that open-ocean a_{CDOM} was lower than the detection limit of conventional spectrophotometers at
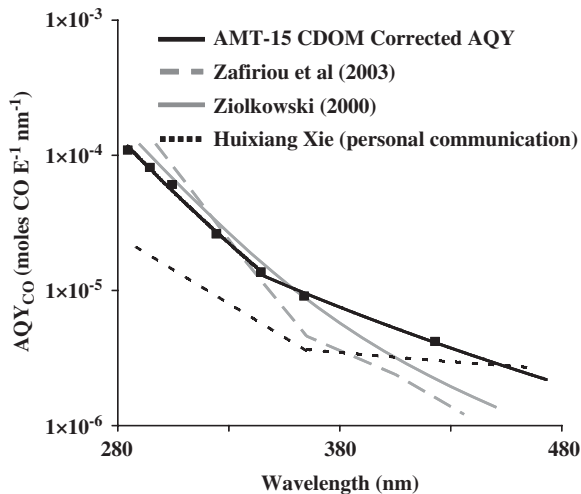
Fig. 5. Spectral variations in carbon monoxide apparent quantum yield (AQY_{CO}). AMT-15 CDOM corrected is the AQY_{CO} spectrum calculated in this study. Solid lines represent the power regressions used to parameterise AQY_{CO} spectral variation. The equation describing the line for 280–440 nm is AQY_{CO} at wavelength $\lambda = 2.70 \times 10^{23(\lambda \times -11.2)}$ ($r^2 = 0.99$). The equation describing the line for 440–800 nm is AQY_{CO} at wavelength $\lambda = 2.75 \times 10^{9(\lambda \times -5.65)}$ ($r^2 = 0.99$). Other AQY_{CO} spectra are for the Pacific Ocean (Zafiriou et al., 2003) and the Atlantic Ocean (Ziolkowski, 2000; Huixiang Xie, personal communication).

wavelengths >360 nm and below instrument precision at wavelengths >400 nm. Secondly, measuring CO production at wavelengths >350 nm for oceanic waters requires long-term irradiations (up to 12 h; Zafiriou et al., 2003) at low chromophore densities, which are apt to underestimate CO formation because CO production rates decrease rapidly with increasing absorbed photon dose (Stubbins, 2001). As discussed above, our AQY_{CO} spectrum is derived from a parameterisation based on riverine, estuarine and coastal AQY_{CO} data. The higher production rates in these samples enabled irradiation times below 4 h, reducing the impact of falling AQY_{CO} with irradiation time (Stubbins, 2001). By contrast, the AQY_{CO} spectrum of Xie (Huixiang Xie, personal communication, 2000; Fig. 5) is lower than our calculated spectrum and those of Zafiriou et al. (2003) and Ziolkowski (2000) at short wavelengths, higher than those of Zafiriou et al. (2003) and Ziolkowski (2000) at wavelengths >430 nm, and higher than all three other spectra at wavelengths >460 nm. We therefore concluded that our own spectrum was within the range of empirical oceanic AQY_{CO} spectra, and a best fit

parameterisation was obtained by splitting the AQY_{CO} spectrum into two sections (285–345 and 345–423 nm) each fitted using a power regression (see Fig. 5 caption, for regression results). This AQY_{CO} spectrum was then used to calculate CO photoproduction via Eq. (1). To assess the influence of variations in published oceanic AQY_{CO} spectra on our rate estimates we also calculated CO photoproduction using the AQY_{CO} spectra of Ziolkowski (2000) and Zafiriou et al. (2003).

3. Results and discussion

Using SMARTS2 irradiance and the CDOM-based AQY_{CO} spectrum described above we estimate CO photoproduction in the Global ocean to be 49 Tg CO-C yr^{-1}. Using SMARTS2 irradiance data and the AQY_{CO} spectra of Zafiriou et al. (2003) and Ziolkowski (2000) yielded rates of 38 and 45 Tg CO-C yr^{-1}, respectively. These latter rates were slightly lower (3–13%) than our own estimate, chiefly due to lower AQY_{CO} at wavelengths >360 nm (Fig. 5). Irradiance data from Leifer (1988) yielded 39 Tg CO-C yr^{-1}, using the AQY_{CO} spectrum of Zafiriou et al. (2003) and 54 Tg CO-C yr^{-1} using both our AQY_{CO} spectrum and that of Ziolkowski (2000). The close agreement between these rates shows that our estimates are not overly sensitive to variations in either AQY_{CO} or irradiance parameterisations.

We further tested the sensitivity of the model towards changes in cloud cover, surface reflectance, and the concentration of photoreactive chromophores. Using the SMARTS2 irradiance data without cloud cover attenuation yielded rates between 47 and 62 Tg CO-C yr^{-1}, and assuming that all chromophores in the ocean were photoreactive (i.e. A_{CDOM} is replaced by A_{CDOM} + particulate absorbance in Eq. (1)) yielded rates between 53 and 84 Tg CO-C yr^{-1}; the latter value represented our highest estimate for CO photoproduction in the open-ocean. Sensitivity to water-surface reflectance was an order of magnitude below that for cloud cover and was therefore regarded as unimportant.

Overall, the highest rates were those calculated using our own AQY_{CO} spectrum, while the lowest rates were obtained with the AQY_{CO} spectrum from Zafiriou et al. (2003). These sensitivity analyses demonstrate that the model was most responsive to the rate of light absorption by photoreactive chromophores, i.e., the partitioning of light absorbance between photoreactive and unreactive

chromophore fractions. Differences between individual photoproduction rate estimates increased, when light absorbed by both CDOM and particulates was assumed to produce CO, because particulates comprised a significant proportion of total absorbance at wavelengths $>360\,nm$, where our own AQY_{CO} are higher than those of Zafiriou et al. (2003). Therefore it is our view that future research into CO photoproduction, and environmental photoreactions generally, should focus upon increasing the coverage of high quality CDOM and particulate absorbance data and also address the photoreactivity of particulate and colloidal organic matter. However, the modest sensitivity of the model output to large variations in input data indicated that our approach was robust, and suggested that Global CO photoproduction falls into the narrow range of 38–84 Tg CO-C yr^{-1}.

We propose that the arithmetic mean of the six model estimates (two irradiance models and three AQY_{CO} spectra), based on cloud cover and the assumption that only CDOM produces CO, can be viewed as the current best estimate of Global oceanic CO photoproduction, i.e. 47 $\pm$ 7 Tg CO-C yr^{-1}. This estimate is at the lower end of previous estimates of oceanic CO photoproduction (30–820 Tg CO-C yr^{-1}; Valentine and Zepp, 1993; Zuo and Jones, 1995; Moran and Zepp, 1997; Siegel, 2001; Zafiriou et al., 2003), and significantly lower than previous estimates based on the extrapolation of CO photoproduction rates from terrestrial (Valentine and Zepp, 1993 (130–170 Tg CO-C yr^{-1}); Moran and Zepp, 1997 (820 Tg CO-C yr^{-1})) and coastal/shelf waters (Zuo and Jones, 1995 (510 Tg CO-C yr^{-1})) to the global ocean. However, recent work showed that oceanic AQY_{CO} spectra (Huixiang Xie, personal communication; Ziolkowski, 2000; Zafiriou et al., 2003) are significantly lower than those for terrestrial (Valentine and Zepp, 1993; Gao and Zepp, 1998; Stubbins, 2001) and even coastal waters (Stubbins, 2001), suggesting that the earlier work may have overestimated oceanic CO photoproduction considerably. Conversely, recent research, using AQY_{CO} spectra from open-ocean waters and a similar rationale to that used here, yielded rates ranging from 30 to 50 Tg CO-C yr^{-1} (Siegel, 2001; Zafiriou et al., 2003), in broad agreement with our best estimate of 47 $\pm$ 7 Tg CO-C yr^{-1}. The agreement between these recent estimates and the limited sensitivity of the presented model towards changes in parameterisations of key variables lend confidence to our current best estimate (47 $\pm$ 7 Tg CO-C yr^{-1}) and lead us to conclude that global open-ocean CO photoproduction should be constrained at the lower end of previous estimates.

We further compared our best estimate of Global CO photoproduction to other CO cycling rates from the literature. Global oceanic CO oxidation in the mixed layer was assumed to be 32 $\pm$ 18 Tg CO-C yr^{-1} (Zafiriou et al., 2003). Global sea–air flux, 6 $\pm$ 5 Tg CO-C yr^{-1}, was taken as the mean of recent estimates based on air–sea gas exchange parameterisations and supersaturation of CO in open-ocean surface waters (Bates et al., 1995; Rhee, 2000; Stubbins et al., 2006). Therefore our best estimate for the combined CO sinks in the mixed-layer was 38 $\pm$ 23 Tg CO-C yr^{-1}, indicating that the mixed-layer CO cycle is broadly balanced within errors. Nevertheless, the difference between sources and sinks also may highlight shortcomings in data coverage or in the assumptions underpinning the source and sink estimates.

A simple estimate of CO fluxes across the pycnocline rules out downward mixing as a significant sink for mixed-layer CO. Assuming mean surface-water CO to be 0.9 nmol L^{-1} (Stubbins et al., 2006), mean deep-water CO to be 0.2 nmol L^{-1} (personal observation), and a diffusion coefficient across the pycnocline (K_z) of 0.11–2.9 cm^{-2} s^{-1} (Law et al., 2003), we estimate the CO flux from the mixed layer to underlying waters to be between 0.1 and 2.6 Tg CO-C yr^{-1}. The upper limit of this range is the maximum possible rate, our view being that the actual rate would likely fall below 1 Tg CO-C yr^{-1}. Alternative explanations include underestimation of microbial CO oxidation rates, which vary considerably with region and water-column depth (Conrad and Seiler, 1980, 1982; Zafiriou et al., 2003), under-estimation of the air–sea gas flux or over-estimation of photoproduction. However, given that the difference between water-column sources and sinks is within the errors of our respective rate estimates, we propose that the system can be regarded as balanced, with all key sources and sinks identified and reasonably constrained. This view is corroborated by Zafiriou et al. (2003), who determined that CO photoproduction in blue waters was roughly balanced by combined sinks due to oxidation and air–sea gas exchange. The rates presented above represent a significant downsizing of the global oceanic CO cycle, constraining oceanic CO turnover at the lower end of previous estimates.

4. Implications for the oceanic carbon cycle

After carbon dioxide, CO is the second most important identifiable product of DOM photodegradation. While CO photoproduction alone is a significant term in marine DOM turnover, the well-constrained relationship between photochemical CO_2 and CO production rates may be used to estimate the total photomineralisation of open-ocean DOC. In order to estimate Global photochemical inorganic carbon (DIC) release from DOC, we adopted a ratio of CO_2:CO photoproduction of 14 (Miller and Zepp, 1995; Gao and Zepp, 1998) and further assumed that the photoproduction of biolabile carbon is approximately 13 times that of CO photoproduction (Miller et al., 2002b). These assumptions are in broad agreement with previous findings that the ratio of DIC photoproduction to photochemical release of biolabile organic carbon is approximately 1 (Miller and Moran, 1997). In this way, combined oceanic DOC photomineralisation was estimated to be approximately $1.3 \, \mathrm{Pg\,C\,yr^{-1}}$, high enough to account for the removal of Global riverine organic carbon inputs to the oceans $(0.4–0.9 \, \mathrm{Pg\,C\,yr^{-1}};$ Prather et al., 2001) and significantly greater than the rate of organic carbon burial in marine sediments $(0.1–0.2 \, \mathrm{Pg\,C\,yr^{-1}};$ Hedges et al., 1997). Assuming a mean annual oceanic primary production of $48 \, \mathrm{Pg\,C\,yr^{-1}}$, calculated as the arithmetic mean of ocean primary production estimates in Longhurst et al. (1995), Field et al. (1998), and Palmer and Totterdell (2001), DOC photomineralisation represents ~3% of primary production. This estimate is significantly lower than previous estimates of photochemical DOC mineralisation to CO_2 and CO by Mopper and Kieber (2000) and Miller and Zepp (1995), which accounted for 10% and 30% of primary production, respectively. However, the estimate of Miller and Zepp (1995) was based on DIC photoproduction rates from riverine, near coastal, and salt marsh environments and very likely overestimated oceanic rates, because CDOM levels and photoreactivity are lower in the open-ocean (Green and Blough, 1994; Stubbins, 2001). Our own estimate of global photochemical DIC release is closer to the previous estimate by Mopper and Kieber (2000), which was based on a similar rationale and a CO photoproduction estimate of $130 \, \mathrm{Tg\,CO\text{-}C\,yr^{-1}}$, the lower limit of global CO photoproduction estimates available at that time (Valentine and Zepp, 1993; Moran and Zepp,

1997; Zuo and Jones, 1995). The difference between our estimate and that of Mopper and Kieber (2000) is principally due to differences in the CO photoproduction data, and can be attributed to the lower, and in our view more realistic, oceanic AQY_{CO} parameterisations used here (Stubbins, 2001; Ziolkowski, 2000; Zafiriou et al., 2003). Based upon this reasoning we believe that the role of photochemistry in the open-ocean C-cycle is significantly lower than previously thought. Nevertheless, it should be noted that our revised estimate of global photochemical DOM turnover is still greater than terrestrial inputs and burial in marine sediments and, if mixing allowed, could remove the entire oceanic DOC pool $(700 \, \mathrm{Pg\,C};$ Hansell and Carlson, 2002) within around 500 years. It is evident therefore that photochemistry should still be regarded as a significant term in the global carbon cycle. Furthermore, our estimate is based on open-ocean regions with low CDOM levels and photoreactivity. It is therefore plausible that the inclusion of additional data from coastal and upwelling regions may lead to moderate upward revisions of estimated global marine DOM turnover. Given that open-ocean photoproduction of CO now appears well-constrained, we propose that further work should focus on coastal waters, upwelling and high latitude regions, where variability in CDOM levels and photoreactivity is highest but data cover remains sparse.

References

Bates, T.S., Kelly, K.C., Johnson, J.E., Gammon, R.H., 1995. Regional and seasonal variations in the flux of oceanic carbon monoxide to the atmosphere. Journal of Geophysical Research 100 (D11), 23093–23101.

Buiteveld, H., Hakvoort, J.H.M., Donze, M., 1994. The optical properties of pure water. In: Jaffe, J.S. (Ed.), Ocean Optics XII. SPIE Proceedings Series. Bergen, Norway, pp. 174–183.

Bullister, J.L., Guinasso, N.L., Schink, D.R., 1982. Dissolved hydrogen, carbon-monoxide, and methane at the CEPEX site. Journal of Geophysical Research 87 (C3), 2022–2034.

Caires, S., Sterl, A., 2005. 100-year return value estimates for ocean wind speed and significant wave height from the ERA-40 data. Journal of Climate 18 (7), 1032–1048.

Conrad, R., Seiler, W., 1980. Photo-oxidative production and microbial consumption of carbon-monoxide in seawater. FEMS Microbiology Letters 9 (1), 61–64.

Conrad, R., Seiler, W., 1982. Utilization of traces of carbon-monoxide by aerobic oligotrophic microorganisms in ocean, lake and soil. Archives of Microbiology 132 (1), 41–46.

Conrad, R., Seiler, W., Bunse, G., Giehl, H., 1982. Carbon monoxide in seawater (Atlantic Ocean). Journal of Geophysical Research 87 (C11), 8839–8852.

Doney, S.C., Najjar, R.G., Stewart, S., 1995. Photochemistry, mixing and diurnal cycles in the upper ocean. Journal of Marine Research 53, 341–369.

Erickson, D.J., 1989. Ocean to atmosphere carbon monoxide flux: global inventory and climate implications. Global Biogeochemical Cycles 3, 305–314.

Field, C.B., Behrenfeld, M.J., Randerson, J.T., Falkowski, P., 1998. Primary production of the biosphere: integrating terrestrial and oceanic components. Science 281 (5374), 237–240.

Gammon, R.H., Kelly, K.C., 1990. Photochemical production of carbon monoxide in surface waters of the Pacific and Indian oceans. In: Blough, N.V., Zepp, R.G. (Eds.), Effects of Solar Ultraviolet Radiation of Biogeochemical Dynamics in Aquatic Environments. Woods Hole Oceanographic Institution, Woods Hole, MA, USA.

Gao, H., Zepp, R.G., 1998. Factors influencing photoreactions of dissolved organic matter in a coastal river of the southeastern United States. Environmental Science and Technology 32, 2940–2946.

Gnanadesikan, A., 1996. Modeling the diurnal cycle of carbon monoxide: sensitivity to physics, chemistry, biology, and optics. Journal of Geophysical Research 101 (C5), 12177–12191.

Green, S.A., Blough, N.V., 1994. Optical absorption and fluorescence properties of chromophoric dissolved organic matter in natural waters. Limnology and Oceanography 39, 1903–1916.

Gueymard, C., 1995. SMARTS2, A simple model of the atmospheric radiative transfer of sunshine: algorithms and performance assessment, Report No. FSEC-PF-270-95, Florida Solar Energy Center.

Hansell, D.A., Carlson, C.A., 2002. Preface. In: Hansell, D.A., Carlson, C.A. (Eds.), Biogeochemistry of Marine Dissolved Organic Matter. Academic Press, London, pp. xxi–xxii.

Hedges, J.I., Keil, R.G., Benner, R., 1997. What happens to terrestrial organic matter in the ocean? Organic Geochemistry 27 (5–6), 195–212.

Johannessen, S., Ziolkowski, L., Miller, W., 2000. Comparison of photochemical production rates of carbon monoxide and dissolved inorganic carbon in the ocean. Paper Presented at Pacifichem 2000. American Chemical Society, Pacifichem, Honolulu, Hawaii.

Johnson, J.E., Bates, T.S., 1996. Sources and sinks of carbon monoxide in the mixed layer of the tropical South Pacific Ocean. Global Biogeochemical Cycles 10 (2), 347–359.

Kettle, A.J., 1994. A model of the temporal and spatial distribution of carbon monoxide in the mixed layer. M.Sc. Thesis, Woods Hole Oceanographic Institution, Institute of Technology Joint Program in Oceanography, Woods Hole, MA, USA, 146pp.

Kettle, A.J., 2005. Diurnal cycling of carbon monoxide (CO) in the upper ocean near Bermuda. Ocean Modelling 8, 337–367.

Kieber, D.J., McDaniel, J.A., Mopper, K., 1989. Photochemical sources of biological substrates in seawater: implications for carbon cycling. Nature 341, 637–639.

Kitidis, V., Stubbins, A.P., Uher, G., Upstill Goddard, R.C., Law, C.S., Woodward, E.M.S., 2006. Variability of chromophoric organic matter in surface waters of the Atlantic Ocean. Deep-Sea Research II, this issue [doi:10.1016/j.dsr2.2006.05.009].

Law, C.S., Abraham, E.R., Watson, A.J., Liddicoat, M.I., 2003. Vertical diffusion and nutrient supply to the surface mixed layer of the Antarctic Circumpolar Current. Journal of Geophysical Research 108 (C8), 3272.

Leifer, A., 1988. The Kinetics of Environmental Aquatic Photochemistry. American Chemical Society, Washington, DC, 336pp.

Longhurst, A., Sathyendranath, S., Platt, T., Caverhill, C., 1995. An estimate of global primary production in the ocean from satellite radiometer data. Journal of Plankton Research 17 (6), 1245–1271.

Miller, W.L., Moran, M.A., 1997. Interaction of photochemical and microbial processes in the degradation of refractory dissolved organic matter from a coastal marine environment. Limnology and Oceanography 42, 1317–1324.

Miller, W.L., Zepp, R.G., 1995. Photochemical production of dissolved inorganic carbon from terrestrial organic-matter: significance to the oceanic organic-carbon cycle. Geophysical Research Letters 22 (4), 417–420.

Miller, R.L., Belz, M., Del Castillo, C., Trzaska, R., 2002a. Determining CDOM absorption spectra in diverse coastal environments using a multiple pathlength, liquid core waveguide system. Continental Shelf Research 22 (9), 1301–1310.

Miller, W.L., Moran, M.A., Sheldon, W.M., Zepp, R.G., Opsahl, S., 2002b. Determination of apparent quantum yield spectra for the formation of biologically labile products. Limnology and Oceanography 47 (2), 343–352.

Mopper, K., Kieber, D.J., 2000. Marine photochemistry and its impact on carbon cycling. In: de Mora, S., Demers, S., Vernet, M. (Eds.), The Effects of UV Radiation in the Marine Environment. Cambridge Environmental Chemistry Series, vol. 10. Cambridge University Press, New York, pp. 101–129.

Moran, M.A., Zepp, R.G., 1997. Role of photoreactions in the formation of biologically labile compounds from dissolved organic matter. Limnology and Oceanography 42, 1307.

Myers, D.R., Emery, K.E., Gueymard, C., 2002. Terrestrial solar spectral modeling tools and applications for photovoltaic devices. Report No. NREL/CP-520-31407. National Renewable Energy Laboratory.

Najjar, R.G., Erickson, D.J., Madronich, S., 1995. Modeling the air–sea fluxes of gases formed from the decomposition of dissolved organic matter: carbonyl sulfide and carbon monoxide. In: Zepp, R.G., Sonntag, C. (Eds.), The Role of Nonliving Organic Matter in the Earth's Carbon Cycle: Report of the Dahlem Workshop on the Role of Nonliving Organic Matter in the Earth's Carbon Cycle, Berlin, 1993. Wiley, New York, pp. 107–132.

Nelson, N.B., Siegel, D.A., Michaels, A.F., 1998. Seasonal dynamics of colored dissolved organic material in the Sargasso Sea. Deep-Sea Research I 45 (6), 931–957.

Palmer, J.R., Totterdell, I.J., 2001. Production and export in a global ocean ecosystem model. Deep-Sea Research I 48 (5), 1169–1198.

Prather, M., Ehhalt, D., Dentener, F., Derwent, R., Dlugokencky, E., Holland, E., Isaksen, I., Katima, J., Kirchhoff, V., Matson, P., Midgley, P., Wang, M., 2001. Atmospheric chemistry and greenhouse gases. In: Houghton, J.T., Ding, Y., Griggs, D.J., Noguer, M., van der Linden, P.J., Dai, X., Maskell, K., Johnson, C.A. (Eds.), Climate Change 2001: The Scientific Basis. Contribution of Working Group 1 to the Third Assessment Report of the Intergovernmental Panel on Climate Change. Cambridge University Press, Cambridge, pp. 239–287 (Chapter 4).

Redden, G.D., 1982. Characteristics of photochemical production of carbon monoxide in seawater. M.Sc. Thesis, Oregon State University, Corvallis, OR, USA.

Rhee, T.S., 2000. The process of air–water exchange and its application. Ph.D. Thesis. A and M University, TX, USA.

Siegel, D.A., 2001. Global distribution and dynamics of chromophoric dissolved organic matter: implications for marine photochemistry. Paper Presented at the Aquatic Sciences Meeting, American Society of Limnology and Oceanography, Waco, TX, USA.

Stubbins, A., 2001. Aspects of aquatic CO photoproduction from CDOM. Ph.D. Thesis, University of Newcastle-upon-Tyne.

Stubbins, A., Uher, G., Kitidis, V., Law, C., Upstill-Goddard, R.C., Woodward, E.M.S., 2006. The open ocean source of atmospheric carbon monoxide. Deep Sea Research II, this issue [doi:10.1016/j.dsr2.2006.05.010].

Valentine, R.L., Zepp, R.G., 1993. Formation of carbon-monoxide from the photodegradation of terrestrial dissolved organic-carbon in natural waters. Environmental Science and Technology 27 (2), 409–412.

Wilson, D.F., Swinnerton, J.W., Lamontagne, R.A., 1970. Production of carbon monoxide and gaseous hydrocarbons in seawater: relation to dissolved organic carbon. Science 168, 1576–1577.

Zafiriou, M.C., Andrews, S.S., Wang, W., 2003. Concordant estimates of oceanic carbon monoxide source and sink processes in the Pacific yield a balanced global "blue-water" CO budget. Global Biogeochemical Cycles 17 (1), 1015, doi:10.1029/2001GB001638.

Zepp, R.G., Cline, D.M., 1977. Rates of direct photolysis in aquatic environments. Environmental Science and Technology 11, 359–366.

Ziolkowski, L.A., 2000. Marine photochemical production of carbon monoxide. M.Sc. Thesis, Dalhousie University, Halifax, NS, Canada, 121pp.

Zuo, Y., Jones, R.D., 1995. Formation of carbon-monoxide by photolysis of dissolved marine organic material and its significance in the carbon cycling of the oceans. Naturwissenschaften 82 (10), 472–474.

Further reading

Mopper, K., Zhou, X.L., Kieber, R.J., Kieber, D.J., Sikorski, R.J., Jones, R.D., 1991. Photochemical degradation of dissolved organic-carbon and its impact on the oceanic carbon-cycle. Nature 353 (6339), 60–62.